Inorganic Chemistry
Article

Inorg. Chem. **2010**, *49*, 2349–2359 **2349**
DOI: 10.1021/ic902225f

Molecular Structure and Electrochemical Behavior of Uranyl(VI) Complex with Pentadentate Schiff Base Ligand: Prevention of Uranyl(V) Cation−Cation Interaction by Fully Chelating Equatorial Coordination Sites

Koichiro Takao,[†,‡] Masaru Kato,[§] Shinobu Takao,[‡] Akira Nagasawa,[§] Gert Bernhard,[‡] Christoph Hennig,[‡] and Yasuhisa Ikeda*[,†]

[†]*Research Laboratory for Nuclear Reactors, Tokyo Institute of Technology, 2-12-1-N1-34, O-okayama, Meguro-ku, Tokyo 152-8550, Japan,* [‡]*Institute of Radiochemistry, Forschungszentrum Dresden-Rossendorf, P.O. Box 51 01 19, 01314 Dresden, Germany, and* [§]*Department of Chemistry, Graduate School of Science and Engineering, Saitama University, 255, Shimo-Okubo, Sakura-ku, Saitama City, Saitama 338-8570, Japan*

Received November 13, 2009

The U^{VI} complex with a pentadentate Schiff base ligand (*N,N′*-disalicylidenediethylenetriaminate = saldien^{2-}) was prepared as a starting material of a potentially stable U^{V} complex without any possibility of $U^{V}O_2^{+}\cdots U^{V}O_2^{+}$ cation−cation interaction and was found in three different crystal phases. Two of them had the same composition of $U^{VI}O_2$(saldien)·DMSO in orthorhombic and monoclinic systems (DMSO = dimethyl sulfoxide, **1a** and **1c**, respectively). The DMSO molecule in both **1a** and **1c** does not show any coordination to $U^{VI}O_2$(saldien), but it is just present as a solvent in the crystal structures. The other isolated crystals consisted only of $U^{VI}O_2$(saldien) without incorporation of solvent molecules (**1b**, orthorhombic). A different conformation of the coordinated saldien^{2-} in **1c** from those in **1a** and **1b** was observed. The conformers exchange each other in a solution through a flipping motion of the phenyl rings. The pentagonal equatorial coordination of $U^{VI}O_2$(saldien) remains unchanged even in strongly Lewis-basic solvents, DMSO and *N,N*-dimethylformamide. Cyclic voltammetry of $U^{VI}O_2$(saldien) in DMSO showed a quasireversible redox reaction without any successive reactions. The electron stoichiometry determined by the UV−vis−NIR spectroelectrochemical technique is close to 1, indicating that the reduction product of $U^{VI}O_2$(saldien) is $[U^{V}O_2(\text{saldien})]^{-}$, which is stable in DMSO. The standard redox potential of $[U^{V}O_2(\text{saldien})]^{-}/U^{VI}O_2$(saldien) in DMSO is −1.584 V vs Fc/Fc^{+}. This U^{V} complex shows the characteristic absorption bands due to f−f transitions in its $5f^1$ configuration and charge-transfer from the axial oxygen to U^{5+}.

1. Introduction

Actinide elements at oxidation states +5 and +6 form a typical "actinyl" ion (MO_2^{n+}) in many cases. This species has a linear O═M═O structure. Due to this structural character, the coordination of additional ligands occurs only in the equatorial plane of MO_2^{n+}.[1,2] The number of the equatorial coordination sites varies between 3 and 6. Uranyl(V) is unusually unstable in solutions due to disproportionation.[1]

Recently, the chemistry of U^{V} has attracted special interest, because this field of actinides is poorly explored. Uranyl(V) carbonate, $U^{V}O_2(CO_3)_3^{5-}$, is currently the solely known stable U^{V} species in aqueous solution.[3] In our previous articles, the electrochemical behavior of U^{VI} complexes with organic ligands [Lewis-basic solvent molecules (L), β-diketonates, Schiff bases] in nonaqueous solvents was studied.[4−6] As a result, two stable U^{V} complexes in nonaqueous systems have been found: $[U^{V}O_2(\text{salophen})\text{DMSO}]^{-}$ in DMSO and $[U^{V}O_2(\text{dbm})_2\text{DMSO}]^{-}$ in DMSO (salophen^{2-} = *N,N′*-disalicylidene-*o*-phenylenediaminate, dbm^{-} = dibenzoylmethanate, DMSO = dimethyl sulfoxide). In the same period, Berthet et al. incidentally obtained a single crystal of

*To whom correspondence should be addressed. Phone: +81 3-5734-3061. E-mail: yikeda@nr.titech.ac.jp.

(1) Katz, J. J.; Seaborg, G. T.; Morss, L. R. *The Chemistry of the Actinide Elements*, 2nd ed.;, Chapman and Hall: London, 1986.

(2) Cotton, S. *Lanthanide and Actinide Chemistry*; John Wilety & Sons Ltd: West Sussex, England, 2006.

(3) (a) Cohen, D. *J. Inorg. Nucl. Chem.* **1970**, *32*, 3535–3530. (b) Wester, D. W.; Sullivan, J. C. *Inorg. Chem.* **1980**, *19*, 2838–2840. (c) Ferri, D.; Grenthe, I.; Salvatore, F. *Inorg. Chem.* **1983**, *22*, 3162–3165. (d) Madic, C.; Hobart, D. E.; Begun, G. M. *Inorg. Chem.* **1983**, *22*, 1494–1503. (e) Mizuguchi, K.; Park, Y.-Y.; Tomiyasu, H.; Ikeda, Y. *J. Nucl. Sci. Technol.* **1993**, *30*, 542–548. (f) Docrat, T. I.; Mosselmans, J. F. W.; Charnock, J. M.; Whiteley, M. W.; Collison, D.; Livens, F. R.; Jones, C.; Edmiston, M. J. *Inorg. Chem.* **1999**, *38*, 1879–1882. (g) Mizuoka, K.; Grenthe, I.; Ikeda, Y. *Inorg. Chem.* **2005**, *44*, 4472–4474. (h) Ikeda, A.; Hennig, C.; Tsushima, S.; Takao, K.; Ikeda, Y.; Scheinost, A. C.; Bernhard, G. *Inorg. Chem.* **2007**, *46*, 4212–4219. (i) Grenthe, I.; Fuger, J.; Konings, R. J. M.; Lemire, R. J.; Muller, A. B.; Nguyen-Trung, C.; Wanner, H.; Forest, I. *Chemical Thermodynamics of Uranium*; North Holland, Elsevier Science Publishers BV: Amsterdam, The Netherlands, 1992. (j) Fanghänel, T.; Neck, V.; Fuger, J.; Palmer, D. A.; Grenthe, I,; Rand, M. H. *Update on the Chemical Thermodynamics of Uranium, Neptunium, Plutonium, Americium and Technetium*; Elsevier Science BV: Amsterdam, The Netherlands, 2003.

Published on Web 01/28/2010

$U^VO_2(OPPh_3)_4(CF_3SO_3)$ ($OPPh_3$ = triphenylphosphine oxide) and determined its structure.[7]

After these findings, the number of publications concerning the U^V chemistry has increased more and more.[8−11] Most works have focused on the preparation, structure determination, and reactivity of the isolated U^V compounds. Summarizing the knowledge and experiences accumulated so far, one can think about what are requirements for stabilization of U^V. The $U^VO_2(CO_3)_3^{5-}$ species is stable only under alkaline conditions and the presence of a large excess of CO_3^{2-} (e.g., pH ≥ 12.0 in 1 M Na_2CO_3).[3] This fact provides us hints for the stabilization of U^V: (1) exclusion of H^+ from a system and (2) prevention of cation−cation interaction (CCI) between $U^VO_2^+$ ions. The former is straightforward, because H^+ is involved in the dissociation of the axial oxygen atoms (O_{ax}) during the disproportionation of U^V.[12] Regarding the second hint, O_{ax} of $U^VO_2^+$ is Lewis-basic enough to coordinate to another $U^VO_2^+$. As a result, CCI, which may initiate the disproportionation, occurs. One of the ways to prevent such an undesired interaction is use of strong complexation, e.g., $U^VO_2(CO_3)_3^{5-}$: $\log \beta_3^\circ = 6.950 \pm 0.360$ (298 K, zero ionic strength), $\log \beta_3 = 13.3 \pm 0.4$ (298 K, 3 M $NaClO_4$).[3c,i,j] The alkaline system with excess CO_3^{2-} satisfies both requirements and consequently results in the stable $U^VO_2(CO_3)_3^{5-}$. If a nonaqueous aprotic solvent is taken instead of water, the first requirement is met. For the second hint, we clarified that a U^V complex with multidentate ligand tends to be more stabilized than those with only unidentate L such as DMSO and DMF.[4,5] Hayton et al.[9] introduced bulky aryl substituents into β-diketiminate ligands to offer steric protection to the $U^VO_2^+$ moiety, which kinetically stabilizes U^V. Mazzanti et al.[10] succeeded in the preparation of several mono- and polynuclear U^V species by using dbm^- and tetradentate Schiff base derivatives which were exactly the same or quite similar to ours mentioned above. In their recent article,[10f] it was stated that fully stable U^V complexes in organic solution can be prepared by a careful tuning of both steric and electronic properties of the supporting ligand coupled to an appropriate choice of counterions. As a common view, the use of a multidentate bulky ligand seems preferable for the protection of $U^VO_2^+$ from undesired reactions like disproportionation and, finally, for the stabilization of U^V. However, a U^V−pyridine solvate complex, $U^VO_2(py)_5^+$, is known as a compound stable under anaerobic conditions.[8a,10a] In connection with this exceptional fact, the necessity of bulky and/or strong coordination for the stability of U^V is still a subject of discussion.[8b] Nevertheless, we believe that full chelation of the equatorial coordination sites of $U^VO_2^+$ with a multidentate ligand is one approach to eliminate the possibility of CCI, and hence, to stabilize U^V.

In our usual method, U^V complexes are prepared using electrochemical reduction of the parent U^{VI} ones in solution, because this technique is superior to the chemical process in precise control of the reaction. In the electrochemical experiment for nonaqueous samples, tetraalkylammonium salts with ClO_4^-, BF_4^-, and PF_6^- are usually taken as supporting electrolytes. Since both of these cations and anions have no or little bonding ability with charged species, no additional interactions between the generated U^V complex and counterion, for instance, the $U^V{=}O_{ax}{-}K^+$ interaction,[8a,10] could occur. Therefore, one does not need to consider selection of an appropriate counterion and can also be liberated from taking account of a possible equilibrium of association/dissociation of the counterion to/from $U^VO_2^+$. This affords an advantage that the U^V complex prepared through this way can be regarded as a simple species in the solution.

We have already studied the redox chemistry of $U^{V/VI}$ complexes with the tetradentate Schiff base ligand, salophen^{2-}, as described above.[5a,b,d] In this system, the equatorial plane was not saturated only by salophen^{2-}, but an additional L was also involved. With a decreasing concentration of L in dichloromethane, dissociation of L in $[U^VO_2(\text{salophen})L]^-$ tends to be more significant. This reaction resulted in a mixture of $[U^VO_2(\text{salophen})L]^-$ and $[U^VO_2(\text{salophen})]^-$ and finally disturbed observation of the "pure" U^V species. To avoid such a situation, full chelation of the equatorial coordination sites is also favorable. As a next step, we shift to a pentadentate ligand. For instance, *N*,*N*′-disalicylidenediethylenetriaminate (saldien^{2-})[13] and superphthalocyanine[14] are promissing candidates. In this study, we selected saldien^{2-} because of the simplicity of preparation and used its U^{VI} complex $[U^{VI}O_2(\text{saldien})$, Chart 1] as a

(4) (a) Lee, S.-H.; Mizuguchi, K.; Tomiyasu, H.; Ikeda, Y. *J. Nucl. Sci. Technol.* **1996**, *33*, 190–192. (b) Mizuguchi, K.; Lee, S.-H.; Ikeda, Y.; Tomiyasu, H. *J. Alloys Compd.* **1998**, *271−272*, 163–167. (c) Kim, S.-Y.; Tomiyasu, H.; Ikeda, Y. *J. Nucl. Sci. Technol.* **2002**, *39*, 160–165. (d) Kim, S.-Y.; Mizuoka, K.; Mizuguchi, K.; Yamamura, T.; Shiokawa, Y.; Tomiyasu, H.; Ikeda, Y. *J. Nucl. Sci. Technol.* **2002**, No. Suppl. 3, 441–444.

(5) (a) Mizuoka, K.; Kim, S.-Y.; Hasegawa, M.; Hoshi, T.; Uchiyama, G.; Ikeda, Y. *Inorg. Chem.* **2003**, *42*, 1031–1038. (b) Mizuoka, K.; Ikeda, Y. *Inorg. Chem.* **2003**, *42*, 3396–3398. (c) Mizuoka, K.; Ikeda, Y. *Radiochim. Acta* **2004**, *92*, 631–635. (d) Mizuoka, K.; Tsushima, S.; Hasegawa, M.; Hoshi, T.; Ikeda, Y. *Inorg. Chem.* **2005**, *44*, 6211–6218.

(6) Takao, K.; Tsushima, S.; Takao, S.; Scheinost, A. C.; Bernhard, G.; Ikeda, Y.; Hennig, C. *Inorg. Chem.* **2009**, *48*, 9602–9604.

(7) Berthet, J.-C.; Nierlich, M.; Ephritikhine, M. *Angew. Chem., Int. Ed.* **2003**, *42*, 1952–1954.

(8) (a) Berthet, J.-C.; Siffredi, G.; Thuery, P.; Ephritikhine, M. *Chem. Commun.* **2006**, 3184–3186. (b) Berthet, J.-C.; Siffredi, G.; Thuery, P.; Ephritikhine, M. *Dalton Trans.* **2009**, 3478–3494.

(9) (a) Hayton, T. W.; Wu, G. *Inorg. Chem.* **2008**, *47*, 7415–7423. (b) Hayton, T. W.; Wu, G. *J. Am. Chem. Soc.* **2008**, *130*, 2005–2014. (c) Hayton, T. W.; Wu, G. *Inorg. Chem.* **2009**, *48*, 3065–3072. (c) Schnaars, D. D.; Wu, G.; Hayton, T. W. *J. Am. Chem. Soc.* **2009**, *131*, 17532–17533. (d) Schettini, M. F.; Wu, G.; Hayton, T. W. *Inorg. Chem.* **2009**, *48*, 11799–11808.

(10) (a) Natrajan, L.; Burdet, F.; Pecaut, J.; Mazzanti, M. *J. Am. Chem. Soc.* **2006**, *128*, 7152–7153. (b) Burdet, F.; Pecaut, J.; Mazzanti, M. *J. Am. Chem. Soc.* **2006**, *128*, 16512–16513. (c) Nocton, G.; Horeglad, P.; Pecaut, J.; Mazzanti, M. *J. Am. Chem. Soc.* **2008**, *130*, 16633–16645. (d) Horeglad, P.; Nocton, G.; Filinchuk, Y.; Pecaut, J.; Mazzanti, M. *Chem. Commun.* **2009**, 1843–1845. (e) Mougel, V.; Horeglad, P.; Nocton, G.; Pecaut, J.; Mazzanti, M. *Angew. Chem., Int. Ed.* **2009**, *48*, 8477–8480. (f) Nocton, G.; Horeglad, P.; Vetere, V.; Pecaut, J.; Dubois, L.; Maldivi, P.; Edelstein, N. M.; Mazzanti, M. *J. Am. Chem. Soc.* DOI: 10.1021/ja9037164.

(11) (a) Arnold, P. L.; Patel, D.; Wilson, C.; Love, J. B. *Nature* **2008**, *451*, 315–317. (b) Graves, C. R.; Kiplinger, J. L. *Chem. Commun.* **2009**, 3831–3853. (c) Arnold, P. L.; Love, J. B.; Patel, D. *Coord. Chem. Rev.* **2009**, *253*, 1973–1978. (d) Fortier, S.; Hayton, T. W. *Coord. Chem. Rev.* **2010**, *254*, 197–214.

(12) (a) Newton, T. W.; Baker, F. B. *Inorg. Chem.* **1965**, *4*, 1166–1170. (b) Ekstrom, A. *Inorg. Chem.* **1974**, *13*, 2237–2241. (c) Steele, H.; Taylor, R. J. *Inorg. Chem.* **2007**, *46*, 6311–6318.

(13) (a) Cattalini, L.; Degetto, S.; Vidali, M.; Vigato, P. A. *Inorg. Chim. Acta* **1972**, *6*, 173–176. (b) Akhtar, M. N.; Smith, A. J. *Acta Crystallogr.* **1973**, *B29*, 275–279. (c) McKenzie, E. D.; Paine, R. E.; Selvey, S. J. *Inorg. Chim. Acta* **1974**, *10*, 41–45. (d) Benetollo, F.; Bombieri, G.; Smith, A. J. *Acta Crystallogr.* **1979**, *B35*, 3091–3093. (e) Bullita, E.; Guerriero, P.; Tamburini, S.; Vigato, P. A. *J. Less-Common Met.* **1989**, *153*, 211–218. (f) Casellato, U.; Guerriero, P.; Tamburini, S.; Vigato, P. A.; Graziani, R. *J. Chem. Soc., Dalton Trans.* **1990**, 1533–1541. (g) Irons, N. J.; Smith, A. J. *Acta Crystallogr.* **1991**, *C47*, 2345–2348. (h) Tamburini, S.; Vigato, P. A.; Guerriero, P.; Casellato, U.; Aguiari, A. *Inorg. Chim. Acta* **1991**, *183*, 81–90.

(14) (a) Day, V. W.; Marks, T. J.; Wachter, W. A. *J. Am. Chem. Soc.* **1975**, *97*, 4519–4527. (b) Cuellar, E. A.; Marks, T. J. *Inorg. Chem.* **1981**, *20*, 3766–3770.

Chart 1

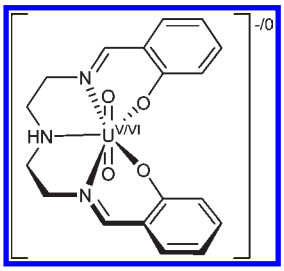

starting material of the corresponding U^V species. The molecular structures of $U^{VI}O_2$(saldien) in the solid and solution states were first studied to confirm if the equatorial plane of U is saturated only by saldien^{2-}, and then the electrochemical behavior of $U^{VI}O_2$(saldien) in DMSO was investigated. Consequently, we succeeded in finding a new stable U^V complex, $[U^VO_2(\text{saldien})]^-$, in DMSO. Recently, we reported its structure determination using X-ray absorption spectroscopy in a communication.[6] In this article, the details of how we found it are described.

2. Experimental Section

Materials. Uranyl(VI) nitrate hexahydrate (1.89 g), diethylenetriamine (0.55 g, Kanto Chemical Co., Ind.), and salicylaldehyde (1.66 g, Fluka) were mixed in ethanol (40 mL). The mixture was refluxed for 40 min and then allowed to cool to room temperature. An orange precipitate was filtered off, washed with ethanol, and dried at room temperature. This compound was dissolved in DMSO (ca. 5 mL, Kanto) heated at 130 °C and recrystallized by cooling it to ambient temperature. The resulting needle-like crystals were of orthorhombic $U^{VI}O_2$(saldien)·DMSO (**1a**). Prismatic crystals of $U^{VI}O_2$(saldien) without any solvent molecules (**1b**) were obtained during the additional storage of the crystals of **1a** upon contact with the mother liquor for several weeks. Platelet crystals of monoclinic $U^{VI}O_2$(saldien)·DMSO (**1c**) also deposited from the same solution ca. 2 months later.

Dimethyl sulfoxide (Kanto) used in the electrochemical and spectroelectrochemical experiments was purified by distillation under a vacuum after drying with CaH_2 (Wako Pure Chemical Ind., Ltd.) and stored over 4A molecular sieves (Wako). Tetra-*n*-butylammonium perchlorate (TBAP, Fluka, electrochemical grade) was used as a supporting electrolyte without further purification. All other chemicals were of reagent grade and used as received.

Characterization. Compounds **1a**−**c** were characterized by using IR, single crystal X-ray diffraction, ^{1}H NMR, and extended X-ray absorption fine structure (EXAFS).

Single crystal X-ray analyses of **1a**−**c** were performed by the following procedure. The single crystal of each compound was mounted on a glass fiber and placed under a low-temperature nitrogen gas stream. Intensity data were collected using an imaging plate area detector in a Rigaku RAXIS RAPID diffractometer with graphite-monochromated Mo Kα radiation (λ = 0.71075 Å). The structures of **1a**−**c** were solved by the SIR92 direct method[15] and expanded using Fourier techniques.[16] All non-hydrogen atoms were anisotropically refined using SHELXL-97.[17] Hydrogen atoms of saldien^{2-} were refined as riding on their parent atoms with $U_{iso}(H) = 1.2U_{eq}(C,N)$. In **1a** and **1c**, the sulfur atom of the solvent DMSO is disordered, and 50% occupancy was given to each S in the structure refinement. Hydrogen atoms of the DMSO molecules in **1a** and **1c** were not located in the structures because of the disorder of S. The final cycle of full-matrix least-squares refinement on F^2 was based on observed reflections and parameters and converged with unweighted and weighted agreement factors, R and wR. All computations were performed with the CrystalStructure crystallographic software package.[18] Crystallographic data and other data collection parameters are summarized in Table 1. Crystallographic information files of **1a**−**c** are available as Supporting Information.

Table 1. Crystallographic Data of Uranyl(VI)−Saldien Complexes

complex	orthorhombic $U^{VI}O_2$(saldien)·DMSO (**1a**)[a]	$U^{VI}O_2$(saldien) (**1b**)	monoclinic $U^{VI}O_2$(saldien)·DMSO (**1c**)
formula	$C_{20}H_{25}N_3O_5SU$	$C_{18}H_{19}N_3O_4U$	$C_{20}H_{25}N_3O_5SU$
fw	657.52	579.39	657.52
cryst syst	orthorhombic	orthorhombic	monoclinic
space group	$Pca2_1$ (#29)	$Pnma$ (#62)	$P2_1/m$ (#11)
a (Å)	20.082(5)	10.464(3)	8.171(2)
b (Å)	10.396(8)	21.617(6)	13.788(3)
c (Å)	10.744(5)	7.976(2)	9.795(3)
β (deg)			101.61(2)
V (Å^3)	2243(2)	1804.2(9)	1081.0(5)
Z	4	4	2
T (K)	173	173	173
D_{calc} (g·cm^{-3})	1.947	2.133	2.020
obsd data (all)	5030	2104	2563
R^b ($I > 2\sigma$)	0.0230	0.0333	0.0194
wR^c (all)	0.0477	0.0780	0.0489
GOF[d]	1.066	1.136	1.085

[a] Flack parameter of **1a** was −0.004(6). [b] $R = \sum||F_o| - |F_c||/\sum|F_o|$. [c] $wR = [\sum(w(F_o^2 - F_c^2)^2)/\sum w(F_o^2)^2]^{1/2}$. [d] GOF $= [\sum w(F_o^2 - F_c^2)^2/(N_o - N_v)]^{1/2}$. A detailed value of the weight (w) in each compound is given in the crystallographic information file attached as Supporting Information.

^{1}H NMR spectra of **1a** and **1c** dissolved in DMSO-d_6 (99 atom %D) were recorded with a JEOL ECX-400 NMR spectrometer (399.78 MHz, external reference: TMS) at different temperatures from 293 to 353 K. The NMR solvent was purchased from ACROS and used as received. A two-dimensional ^{1}H−^{1}H COSY spectrum of **1a** dissolved in a DMSO-d_6 solution was measured at 313 K using the same instrument (1024 slices × 1024 points).

X-ray absorption fine structure (XAFS) spectroscopy was performed at the Rossendorf Beamline (ROBL) BM20 at the European Synchrotron Radiation Facility (ESRF, 6 GeV; 70−90 mA).[19] A Si(111) double-crystal monochromator was employed in channel-cut mode to monochromatize a white X-ray from the synchrotron. Uranium L_{III}-edge X-ray absorption spectra of crystalline **1a** dispersed in a PTFE matrix and solution samples of **1a** (solvent: DMSO, DMF) were recorded in transmission mode using Ar-filled ionization chambers at ambient temperature (295 K) and pressure. The X-ray energy in each experimental run was calibrated by Y foil (fist inflection point at 17038 eV). The threshold energy, $E_{k=0}$, of the U L_{III} edge was defined at 17185 eV. The X-ray absorption spectrum of each sample was accumulated twice and merged. The obtained spectra were processed using Athena for background removal

(15) Altomare, A.; Cascarano, G.; Giacovazzo, C.; Guagliardi, A. *J. Appl. Crystallogr.* **1993**, *26*, 343–350.
(16) Beurskens, P. T.; Admiraal, G.; Beurskens, G.; Bosman, W. P.; Gelder, de R.; Israel, R.; Smits, J. M. M. *DIRDIF99*; Technical Report of the Crystallography Laboratory, University of Nijmegen: Nijmegen, The Netherlands, 1999.
(17) Sheldrick, G. M. *SHELXL-97*; University of Göttingen: Göttingen, Germany, 1997.
(18) *CrystalStructure 3.10*; Rigaku and rigaku/MSC: Tokyo, Japan, 2000−2002.
(19) Reich, T.; Bernhard, G.; Geipel, G.; Funke, H.; Hennig, C.; Rossberg, A.; Matz, W.; Schell, N.; Nische, H. *Radiochim. Acta* **2000**, *88*, 633–637.

and the extraction of EXAFS spectra and Artemis for the EXAFS curve fit.[20] The curve fit was performed in the *R* space, using phases and amplitude calculated by *FEFF* 8.20.[21] The molecular structure of $U^{VI}O_2$(saldien) in **1a** from the single crystal X-ray analysis was used as an initial structure model for the phase and amplitude functions. Single-scattering paths from oxygen, nitrogen, and carbon and multiple-scattering paths from the linear uranyl moiety were included in the EXAFS curve fit. The amplitude decay factor, S_0^2, was fixed at 0.9, and the shifts in the threshold energy, ΔE_0, were constrained to be the same value for all shells.

IR spectra of **1a**−**c** dispersed in KBr matrices were recorded with a diffuse reflectance method by using SHIMADZU FTIR-8400S spectrophotometer. IR Data (KBr, cm^{-1}). **1a**: 895s (O═U═O asymmetric stretching, ν_3), 1040br (S═O stretching, $\nu_{S=O}$), 1627s (C═N stretching, $\nu_{C=N}$), and 3247s (N−H stretching, ν_{N-H}). **1b**: 897s (ν_3), 1629s ($\nu_{C=N}$), and 3247s (ν_{N-H}). **1c**: 891s (ν_3), 1040br ($\nu_{S=O}$), 1624s ($\nu_{C=N}$), and 3202 ms (ν_{N-H}).

Electrochemical and Spectroelectrochemical Experiments. Cyclic voltammetry (CV) measurements were performed at 298 K under a dry argon atmosphere using BAS ALS660B. A three-electrode system consisted of a Pt disk working electrode (electrode surface area: 0.020 mm^2), a Pt wire counter electrode, and a Ag/AgCl reference electrode (3 M NaCl) with the liquid junction filled with 0.1 M TBAP. A ferrocene/ferrocenium ion redox couple (Fc/Fc^+) was taken as the internal reference redox system.[22] Dissolved O_2 in the sample solutions was removed by passing Ar gas through for at least 10 min prior to starting experiments.

UV−vis−NIR spectroelectrochemical measurements for $U^{VI}O_2$(saldien) in DMSO was performed with a SHIMADZU UV-3150 spectrophotometer equipped with an optical transparent thin layer electrode (OTTLE) cell.[23] The optical path length of the cell ($l = 1.89 \times 10^{-2}$ cm) was calibrated spectrophotometrically. The three-electrode system was the same as that in the CV experiment with a replacement of the working electrode by a Pt gauze (80 mesh). The applied potential on OTTLE was controlled by BAS ALS660B. The electronic spectrum at each potential was recorded after equilibrium of the electrochemical reaction, which was completed within 2 min. The sample solutions in the OTTLE cell were deoxygenated by passing dry Ar gas through at least 1 h prior to the experiment.

3. Results and Discussion

3.1. Structure Determination. Orange needle-like crystals first deposited from the DMSO solution dissolving the product obtained from the reaction of $UO_2(NO_3)_2 \cdot 6H_2O$ with diethylenetriamine and salicylaldehyde in ethanol. This crystalline material was characterized as $U^{VI}O_2$(saldien)·DMSO (**1a**) in the orthorhombic system, $Pca2_1$. Inclusion of DMSO was also checked by the characteristic IR peak of $\nu_{S=O}$ at 1040 cm^{-1}. The ORTEP drawing of **1a** is shown in Figure 1. The crystallographic data and selected structural parameters of this compound are listed in Tables 1 and 2, respectively. The U atom in **1a** is seven-coordinated. Two axial oxygens, O_{ax}, are placed at the axial positions, and five coordinating atoms from saldien^{2-} (two O and three N) are located in the equatorial plane. This results in the pentagonal

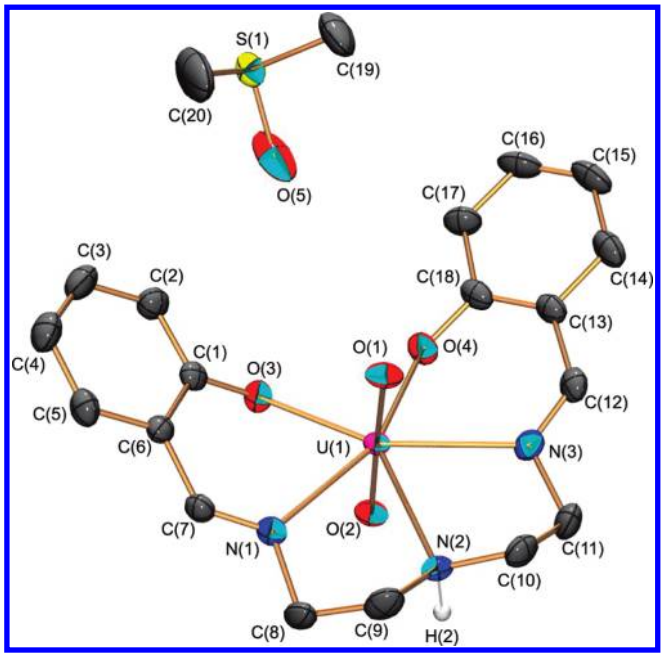

Figure 1. ORTEP drawing of orthorhombic $U^{VI}O_2$(saldien)·DMSO (**1a**) showing 50% probability displacement ellipsoids. Hydrogen atoms other than H(2), which shows the hydrogen bond in the crystal structure, are omitted for clarity. A sulfur atom in DMSO is disordered in 50% occupancy, and one of them, S(1), is only shown in this figure.

bipyramidal coordination sphere around U. The U═O_{ax} bond distances are U(1)−O(1) = 1.788(3) Å and U(1)−O(2) = 1.790(3) Å, which are well comparable with other U^{VI} compounds. The bond distances between U and O of saldien^{2-} [U(1)−O(3), U(1)−O(4): mean 2.23 Å] are similar to those of the reported U^{VI}−Schiff base complexes.[13b,d,g,h,24] The bond distances between U and N are ca. 2.59 Å, which are longer than the U−O distances in the equatorial plane. The $U^{VI}O_2^{2+}$ moiety is slightly bent in the direction of N(2) [O(1)−U(1)−O(2) = 176.2(2)°]. The dihedral angles of the ethylene moieties, N(1)−C(8)−C(9)−N(2) and N(2)−C(10)−C(11)−N(3), are almost equal to 60° [59.6(5)° and 58.4(6)°, respectively], indicating *gauche* geometry. Since the conformational energy for the rotation around the C−C bond axis shows the local minimum at *gauche*, it is reasonable to consider that these parts of saldien^{2-} have sterically favorable shapes in **1a**.

Packing views of **1a** along all axes are shown in Figure S1 (Supporting Information). An intermolecular hydrogen bond was observed between N(2)−H(2) and O(1)^{i} of the neighboring $U^{VI}O_2$(saldien) complexes [symmetry code: (i) $-x, -y + 2, z - 1/2$], as displayed in Figure S2 (Supporting Information). The geometric parameters of this hydrogen bond are listed in Table 3. This intermolecular interaction results in one-dimensional stacking of the $U^{VI}O_2$(saldien) molecules in the crystal structure. A packing diagram of **1a** along the *c* axis is depicted in Figure 2. In this figure, the molecular columns of $U^{VI}O_2$-(saldien) binding through the hydrogen bonds form a channel in the direction of the *c* axis. Each channel is filled

(20) Ravel, B.; Newville, M. *J. Synchrotron Radiat.* **2005**, *12*, 537–541.
(21) Ankudinov, A. L.; Ravel, B.; Rehr, J. J.; Conradson, S. D. *Phys. Rev. B* **1998**, *58*, 7565–7576.
(22) Gritzner, G.; Kůta, J. *Pure Appl. Chem.* **1984**, *56*, 461–466.
(23) (a) DeAngelis, T. P.; Heineman, W. R. *J. Chem. Educ.* **1976**, *53*, 594–597. (b) Heineman, W. R. *J. Chem. Educ.* **1983**, *60*, 305–308. (c) Lin, X. Q.; Kadish, K. M. *Anal. Chem.* **1985**, *57*, 1498–1501. (d) Endo, A.; Mochida, I.; Shimizu, K.; Satô, G. P. *Anal. Sci.* **1995**, *11*, 457–459.
(24) (a) Takao, K.; Ikeda, Y. *Inorg. Chem.* **2007**, *46*, 1550–1562. (b) Cametti, M.; Ilander, L.; Rissanen, K. *Inorg. Chem.* **2009**, *48*, 8632–8637. (c) Fleck, M.; Hazra, S.; Majumder, S.; Mohanta, S. *Cryst. Res. Technol.* **2008**, *43*, 1220–1229.

Table 2. Selected Structural Parameters of Uranyl(VI)-Saldien Complexes

orthorhombic $U^{VI}O_2$(saldien)·DMSO (**1a**)					
Bond Distances (Å)					
U(1)−O(1)	1.788(3)	U(1)−O(3)	2.231(3)	U(1)−N(1)	2.586(4)
U(1)−O(2)	1.790(3)	U(1)−O(4)	2.220(4)	U(1)−N(2)	2.581(4)
				U(1)−N(3)	2.602(3)
Bond Angle (deg)					
O(1)−U(1)−O(2)	176.2(2)				
Dihedral Angle (deg)					
N(1)−C(8)−C(9)−N(2)	59.6(5)	N(2)−C(10)−C(11)−N(3)	58.4(6)		
$U^{VI}O_2$(saldien) (**1b**)					
Bond Distance (Å)					
U(1)−O(1)	1.786(6)	U(1)−O(3)	2.249(4)	U(1)−N(1)	2.569(6)
U(1)−O(2)	1.788(7)			U(1)−N(2)	2.562(7)
Bond Angle (deg)					
O(1)−U(1)−O(2)	175.9(3)				
Dihedral Angle (deg)					
N(1)−C(8)−C(9)−N(2)	56.2(7)				
monoclinic $U^{VI}O_2$(saldien)·DMSO (**1c**)					
Bond Distance (Å)					
U(1)−O(1)	1.780(3)	U(1)−O(3)	2.237(2)	U(1)−N(1)	2.582(3)
U(1)−O(2)	1.783(3)			U(1)−N(2)	2.574(4)
Bond Angle (deg)					
O(1)−U(1)−O(2)	177.1(1)				
Dihedral Angle (deg)					
N(1)−C(8)−C(9)−N(2)	54.8(3)				

Table 3. Hydrogen Bond Geometry

D−H···A	D−H /Å	H···A /Å	D···A /Å	D−H···A /deg
Orthorhombic $U^{VI}O_2$(saldien)·DMSO (**1a**)[a]				
N(2)−H(2)···O(1)^{i}	0.930	2.019	2.935(4)	168.0
$U^{VI}O_2$(saldien) (**1b**)[b]				
N(2)−H(2)···O(2)^{i}	0.930	2.756	3.440(9)	131.2
N(2)−H(2)···O(3)^{i}	0.930	2.738	3.540(7)	144.9
N(2)−H(2)···O(3)^{ii}	0.930	2.738	3.540(7)	144.9
Monoclinic $U^{VI}O_2$(saldien)·DMSO (**1c**)				
N(2)−H(1)···O(4)	0.923	1.986	2.902(4)	171.4

[a] Symmetry code: (i) $-x, -y+2, z-1/2$. [b] Symmetry code: (i) $x+1/2, -y+1/2, -z+1/2$, (ii) $x+1/2, y, -z+1/2$.

with the solvent DMSO molecules, of which sulfur atoms are disordered. The DMSO molecules in the channels are packed in a head-to-tail manner; that is, O(5) is directed to S(1,2) of the neighboring molecule. The distance between O(5) and middle point of the disordered S(1)^{ii} and S(2)^{ii} [symmetric code: (ii) $-x+1/2, y, z-1/2$] is 4.04 Å, which is too long to be assigned to any interaction [cf. sum of van der Waals radii of O and S = 1.52 + 1.80 = 3.32 Å].[25] The space group and lattice constants of **1a** [$Pca2_1$, a = 20.082(5), b = 10.396(8), and c = 10.744(5) Å] are similar to those of the ethanol solvate, $U^{VI}O_2$(saldien)·ethanol, reported previously [$Pca2_1$, a = 9.912(10), b = 11.438(19), and c = 19.599(38) Å].[13g] The similarity of these structures indicates that the channel enables the access of various kinds of solvent molecules.

Upon contact with the DMSO mother liquor, the needle-like crystals of **1a** gradually turned to a new prismatic phase (**1b**) after several weeks. As a result of the single crystal X-ray analysis, **1b** was found to consist of only $U^{VI}O_2$(saldien) without any solvent molecules. A similar conversion from the acetonitrile solvate of $U^{VI}O_2$(saldien) was observed by McKenzie et al.[13c] The molecular structure, crystallographic data, and selected structural parameters of **1b** are shown in Figure 3 and Tables 1 and 2, respectively. The molecular structure of $U^{VI}O_2$(saldien) in **1b** is quite similar to that in **1a** as follows: the pentagonal bipyramidal coordination around U, the typical U=O_{ax} bond distances (mean: 1.79 Å), the slightly bent $U^{VI}O_2^{2+}$ moiety in the direction of N(2) [O(1)−U(1)−O(2) = 175.9(3)°], and the bond distances between U and the coordinating atoms of saldien^{2-} [U−O(3) = 2.249(4) Å, U−N(mean) = 2.56 Å]. A mirror plane

(25) Bondi, A. *J. Phys. Chem.* **1964**, *68*, 441–451.

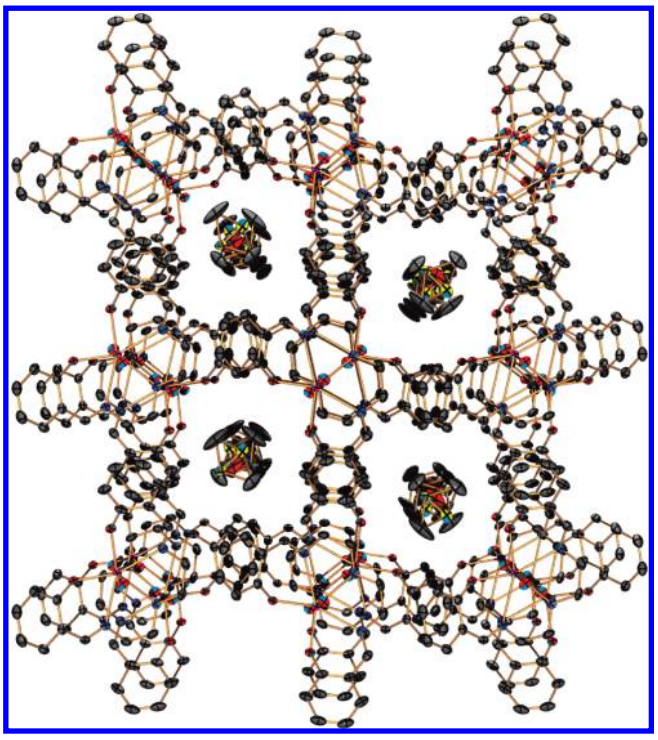

Figure 2. Packing diagram of **1a** along the *c* axis. Hydrogen atoms are omitted for clarity.

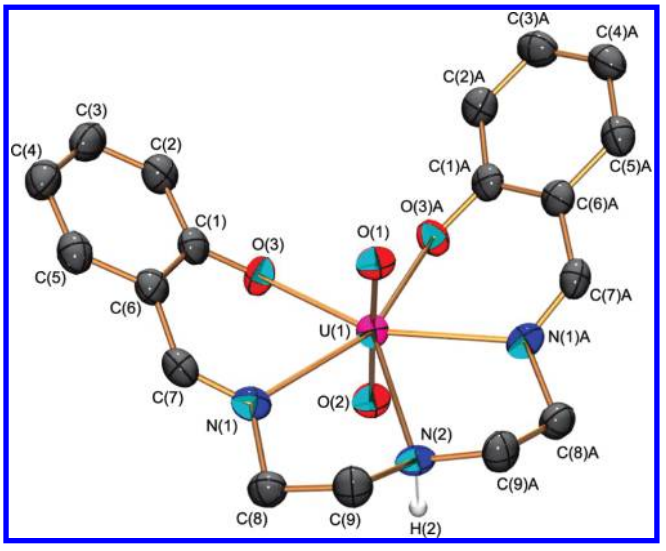

Figure 3. ORTEP drawing of orthorhombic $U^{VI}O_2$(saldien) (**1b**) showing 50% probability displacement ellipsoids. Hydrogen atoms other than H(2), which shows the hydrogen bond in the crystal structure, are omitted for clarity. Symmetry code A: $x, -y + 1/2, z$.

(symmetry code: $x, -y + 1/2, z$) is located through U, O_{ax}, and N(2). The dihedral angle of N(1)−C(8)−C(9)−N(2) [56.2(7)°] indicates the *gauche* conformation of this moiety.

Packing views of **1b** along all axes are shown in Figure S3 in the Supporting Information. The hydrogen bonds between the neighboring complexes are found in N(2)−H(2)···O(2)^{i}, N(2)−H(2)···O(3)^{i}, and N(2)−H(2)···O(3)^{ii} [symmetry codes: (i) $x + 1/2, -y + 1/2, -z + 1/2$, (ii) $x + 1/2, y, -z + 1/2$] as displayed in Figure S4 (Supporting Information). The hydrogen bond geometric parameters of **1b** are summarized in Table 3. The

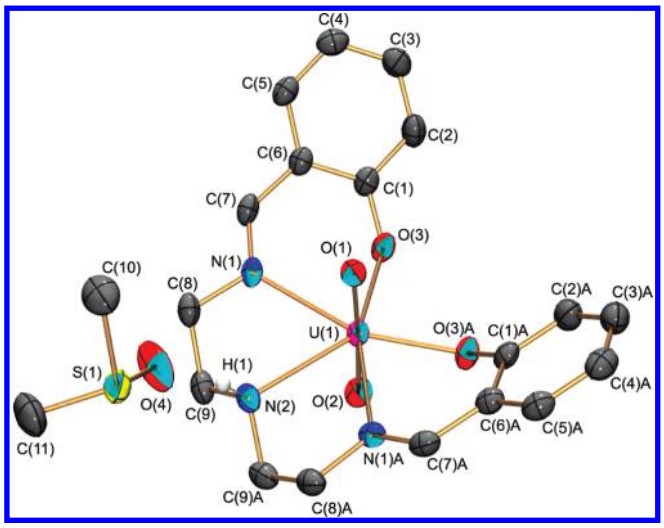

Figure 4. ORTEP drawing of monoclinic $U^{VI}O_2$(saldien)·DMSO (**1c**) showing 50% probability displacement ellipsoids. Hydrogen atoms other than H(1), which shows the hydrogen bond with O(4) of DMSO, are omitted for clarity. A sulfur atom of DMSO is expanded by the plane symmetry and disordered (i.e., 50% occupancy). Only S(1) is shown in this figure. Symmetry code A: $x, -y + 1/2, z$.

intermolecular hydrogen bonds between the neighboring complexes seem to be weak, because the H···O and D···A distances (ca. 2.74 and 3.50 Å, respectively) of **1b** are longer than those in **1a** and **1c** (described below). These hydrogen bonds in **1b** connect the $U^{VI}O_2$(saldien) molecules with each other and form a twisted head-to-tail one-dimensional chain in the crystal structure (Figure S4, Supporting Information).

The crystallographic data of **1b** are almost identical to those of the same compound reported by Smith et al.[13b,d] However, there are several differences in the structural parameters. According to Smith et al., the U=O_{ax} bond distance interacting with the N−H group of the neighboring complex is 1.80(1) Å, which is longer than that without such an interaction [1.74(1) Å]. They mentioned that the asymmetry of the $U^{VI}O_2^{2+}$ moiety could arise from inter- and intramolecular contacts of one of the O_{ax}'s with the N−H groups in the same and neighboring molecules. In contrast, such a difference in the U=O_{ax} bond distances is not found in the present study, as shown in Table 2. Since the X-ray diffraction of **1b** in this study was recorded at a low temperature (173 K) and gave the smaller esd's in the structural parameters, our experiments should provide more precise results than the previous one.

When the crystals of **1b** were stored in the mother liquor, they were converted to platelet crystals of **1c** ca. 2 months later. According to the single crystal X-ray analysis, this compound consists of $U^{VI}O_2$(saldien)·DMSO, which is the same as **1a**, but the crystal system is monoclinic ($P2_1/m$). Thus, **1a** and **1c** are isomorphous. Incorporation of DMSO was also confirmed by the presence of $\nu_{S=O}$ at 1040 cm^{-1} in the IR spectrum. The molecular structure of **1c** is displayed in Figure 4. The crystallographic data and selected structural parameters are listed in Tables 1 and 2, respectively. At first sight, the molecular structure of **1c** is quite similar to those of **1a** and **1b**. The U=O_{ax} bond distances are 1.78 Å (mean), and the bond distances between U and the coordinating

atoms of saldien^{2-} are 2.237(2) Å [U(1)−O(3)] and 2.58 Å [U(1)−N(mean)]. The $U^{VI}O_2^{2+}$ moiety is slightly bent [O(1)−U(1)−O(2) = 177.1(1)°] in the direction of the coordination of N(2). Although the dihedral angle of N(1)−C(8)−C(9)−N(2) [54.8(3)°] is slightly smaller than the corresponding values in **1a** and **1b**, the conformation of this moiety in **1c** is still considered to be *gauche*. A mirror plane (symmetry code: x, $-y + 1/2$, z) is located across U, O_{ax}, N(2), O(4), C(10), and C(11), in which the latter three atoms belong to DMSO. The sulfur atom of DMSO is expanded by this mirror plane, resulting in its disorder in a similar manner to that in **1a**. In the crystal structure of **1c**, the molecular arrangement and the intermolecular interaction are different from those in **1a** in spite of the same composition. The intermolecular hydrogen bond is formed between N(2)−H(1) of saldien^{2-} and O(4) of DMSO. The geometric parameters of this interaction are summarized in Table 3. The hydrogen bond between N−H and O of DMSO is correlated to the N−H stretching, ν_{N-H}. The ν_{N-H} IR frequency of **1c** (3202 cm^{-1}) is smaller than those in **1a** and **1b** (both 3247 cm^{-1}). This arises from the fact that the bond strength between N and H in **1c** is weakened by the hydrogen bond formation.

Packing diagrams of **1c** along all axes are shown in Figure S5 (Supporting Information). Zigzag layers of $U^{VI}O_2$(saldien) molecules which are connected through CH(sp^3)/π interaction between C(9)−H(9B) and the spatially adjacent phenyl ring of neighboring $U^{VI}O_2$(saldien) are found in the packing view along the c axis (distance between C(9) and centroid of the phenyl ring: 3.50 Å, Figure S6, Supporting Information).[26]

The most significant difference in the molecular structure of $U^{VI}O_2$(saldien) in **1a**−**c** is the conformation of saldien^{2-}. When the ethylene moieties of $U^{VI}O_2$(saldien) are put in the upper side of the equatorial plane as shown in Figure 5, the phenyl rings in **1a** and **1b** are directed to the same side of the equatorial plane, while those in **1c** are in the opposite side. It should be reminded that no remarkable differences were detected in the *gauche* form of the ethylene moieties in all compounds. In the crystal structures of **1a** and **1b**, no specific interactions except for the hydrogen bonds through the >NH group were observed, while the CH(sp^3)/π interaction was found in that of **1c**. Hence, the presence and absence of the latter effect would be one of the driving forces of the occurrence of the different conformer in **1c**. The observed conformers of $U^{VI}O_2$(saldien) may exchange with each other in a solution through a flipping motion of (i) the ethylene moieties or (ii) the phenyl rings from one side to the other side of the equatorial plane. A similar reaction is reported for the other U^{VI}−Schiff base complexes.[27]

To study the conformation of $U^{VI}O_2$(saldien) in solution, ^{1}H NMR spectra of **1a** and **1c** dissolved in DMSO-d_6 solutions were measured. The results for **1a** and **1c** are shown in Figures S7 and S8 (Supporting Information), respectively. As a consequence, both spectra are mutually identical to each other, indicating that the rapid exchange reaction between the conformers is taking place. At 313 K, ^{1}H NMR signals were observed at 3.38 (2H, q × d, methylene), 4.09 (2H, d, methylene), 4.57 (4H, m, methylene), 6.66 (2H, t, phenyl), 6.78 (1H, t, >NH), 6.90 (2H, d, phenyl), 7.54 (4H, m, phenyl), and 9.50 ppm (2H, s, −N=CH−). These assignments are in line with the previous reports of similar compounds.[13f,24a] The NMR signal of the >NH group significantly shifts to an upper field from 6.86 ppm (293 K) to 6.61 ppm (353 K) with elevating temperature, suggesting the formation and breakage of the hydrogen bond between >NH and solvent DMSO like that found in the crystal structure of **1c**. At 313 K, this signal is most largely separated from others. If the exchange reaction between the conformers proceeds through the ethylene flipping motion, the chemical exchange between *endo* and *exo* protons will be observed, as shown in Scheme 1. For this discussion, it is necessary to examine if the *endo* and *exo* protons are

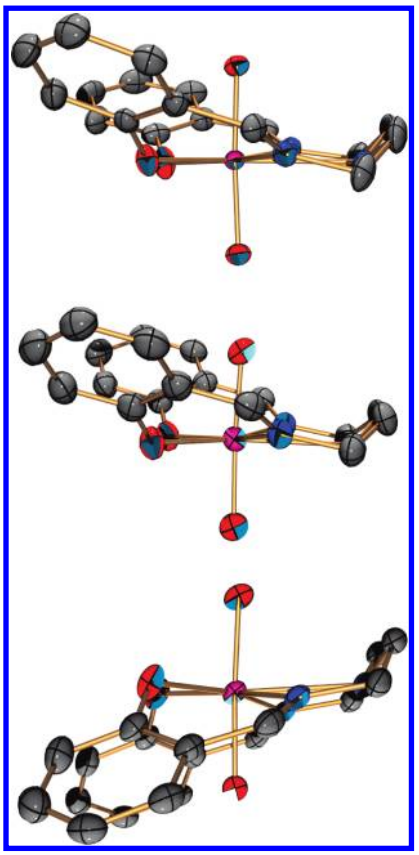

Figure 5. Side views of molecular structures of $U^{VI}O_2$(saldien) in **1a** (top), **1b** (middle), and **1c** (bottom) showing 50% probability displacement ellipsoids. Hydrogen atoms are omitted for clarity.

Scheme 1. Conformer Exchange in Newman Projections along C−C Bond in Ethylene Moiety of $U^{VI}O_2$(saldien)

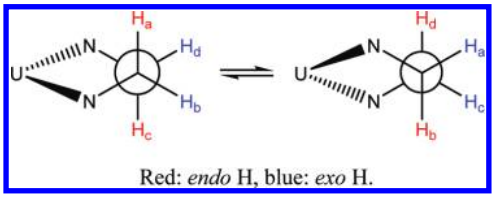

(26) (a) Kobayashi, Y.; Kurasawa, T.; Kinbara, K.; Saigo, K. *J. Org. Chem.* **2004**, *69*, 7436–7441. (b) Tsuzuki, S.; Honda, K.; Uchimaru, T.; Mikami, M.; Fujii, A. *J. Phys. Chem. A* **2006**, *110*, 10163–10168.

(27) (a) Dalla Cort, A.; Mandolini, L.; Palmieri, G.; Pasquini, C.; Schiaffino, L. *Chem. Commun.* **2003**, 2178–2179. (b) Dalla Cort, A.; Gasparrini, F.; Lunazzi, L.; Mandolini, L.; Mazzanti, A.; Pasquini, C.; Pierini, M.; Rompietti, R.; Schiffino, L. *J. Org. Chem.* **2005**, *70*, 8877–8883. (c) Dalla Cort, A.; Mandolini, L.; Pasquini, C.; Shiaffino, L. *J. Org. Chem.* **2005**, *70*, 9814–9821. (d) Ciogli, A.; Dalla Cort, A.; Gasparrini, F.; Lunazzi, L.; Mandolini, L.; Mazzanti, A.; Pasquini, C.; Pierini, M.; Shiaffino, L.; Yafteh Mihan, F. *J. Org. Chem.* **2008**, *73*, 6108–6118.

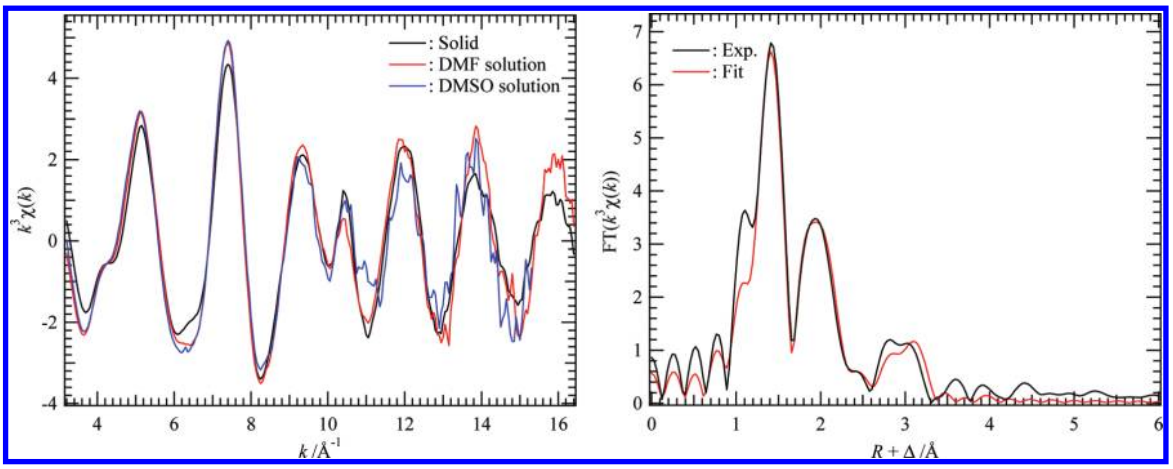

Figure 6. k^3-weighted U L_{III}-edge EXAFS spectra of $U^{VI}O_2$(saldien) in the solid state (**1a**), DMF, and DMSO solutions (left) and Fourier transform of the EXAFS spectrum of the DMSO solution (right).

separately observed or not. Figure S9 shows the $^1H-^1H$ COSY diagram of the DMSO solution dissolving **1a** at 313 K. Correlations of the signals at 3.38 and 4.09 ppm with that at 6.78 ppm of the >NH group were observed. This indicates that these signals are attributable to the methylene group vicinal to >NH. In contrast, the multiplet signal centered at 4.57 ppm does not show any correlation with >NH, but with the −N=CH− group at 9.50 ppm, implying that this multiplet signal arises from the methylene group neighboring on −N=CH−. As shown in the Newman projections along N−C and C−C bonds (Scheme S1, Supporting Information), the *endo* H_a has the possibility of *J*-coupling with the geminal H_b and vicinal ones in two *anti* and one *gauche* conformations, while three *gauche* conformations are found around the *exo* H_b. Usually, the coupling constant (*J*) for the *anti* conformation is ca. 10 Hz, whereas that for *gauche* is smaller (0−5 Hz).[28] Therefore, it should be possible to distinguish the *endo* and *exo* protons from the coupling scheme. As shown in Figure S10 (Supporting Information), the NMR simulation[29] fits very well with the related part of the observed spectrum. The simulated *J* values (Table S1, Supporting Information) are in agreement with those of a similar U^{VI} complex reported elsewhere.[13f] Consequently, it was confirmed that the *endo* (3.38 ppm) and *exo* protons (4.09 ppm) of the methylene group vicinal to >NH are distinguished at 313 K. In addition, we performed Lorentz deconvolution for the ^1H NMR signal of the *endo* H_a and *exo* H_b at different temperatures in Figure S7 (Supporting Information). The estimated full widths at half maxima (fwhm) of them are summarized in Table S2 (Supporting Information). If H_a and H_b exchange with each other through Scheme 1, the rate of this reaction tends to be faster with elevating temperature, resulting in line-broadening, and finally, coalescence of these signals. However, the experimental observation is the opposite; i.e., fwhm decreases slightly with increasing temperature. This means that Scheme 1 does not virtually proceed. Nevertheless, the exchange reaction between the conformers rapidly occurs in the solution. Thus, the mechanism of this reaction is considered to be the flipping motion of the phenyl groups. This exchange mechanism was also proposed for the U^{VI}−salophen complex and its derivatives by Dalla Cort et al.[27] As a matter of fact, the multiplet centered at 7.54 ppm shows spectral change as displayed in Figure S11 (Supporting Information) with increasing temperature, suggesting that the phenyl ring flipping is taking place. Because of complexity of the temperature dependence of this multiplet, further kinetic analysis has not been done.

The most important point in this section is to figure out if L is coordinated or not. In the crystal structures of **1a** and **1c**, one of the strongly Lewis basic L's, DMSO, was incorporated. Especially for **1a**, the potentially coordinating oxygen atom, O(5), is directed toward U(1). However, the interatomic distance between U(1) and O(5) in **1a** (Figure 1) is 6.00 Å, which is too long to regard it as chemical bonding (cf. sum of van der Waals radii of U and O: 1.86 + 1.52 = 3.38 Å).[25] In **1c**, the oxygen atom of DMSO interacts only with N(2)−H(1) through the hydrogen bond, and no coordination possibility of DMSO to U is observable. Therefore, the exclusion of L from the equatorial plane of U^{VI} using the pentadentate ligand was successfully done, as we expected. In the next step, the molecular structure of $U^{VI}O_2$(saldien) in solution has also to be clarified, because U^V will be electrochemically prepared in solution. For this objective, EXAFS spectra of the DMSO and DMF solutions dissolving **1a** were recorded. The k^3-weighted EXAFS spectra are shown in Figure 6 together with that of crystalline **1a** in the PTFE matrix. Although there are minor differences among these spectra, the main features of the EXAFS oscillation are the same. This implies the molecular structure of $U^{VI}O_2$(saldien) in the solid state remains unchanged in both solutions. The right part of Figure 6 shows a Fourier transform of the DMSO solution and the best result of the EXAFS curve fit. The evaluated structural parameters are summarized in Table S3 (Supporting Information).[30] The interatomic distances (*R*) are in agreement with those of $U^{VI}O_2$(saldien) in crystalline **1a**. Furthermore, in accordance with the derived coordination numbers (*N*), the equatorial plane of $U^{VI}O_2^{2+}$ seems to fully chelate

(28) Karplus, M. *J. Am. Chem. Soc.* **1963**, *85*, 2870–2871.
(29) *gNMR*, version 5.0.4.0; Adept Scientific Inc.: Bethesda, MD, 1988−2003.
(30) The structural parameters derived from the EXAFS curve fit for $U^{VI}O_2$(saldien) were reported in our recent communication, ref 6.

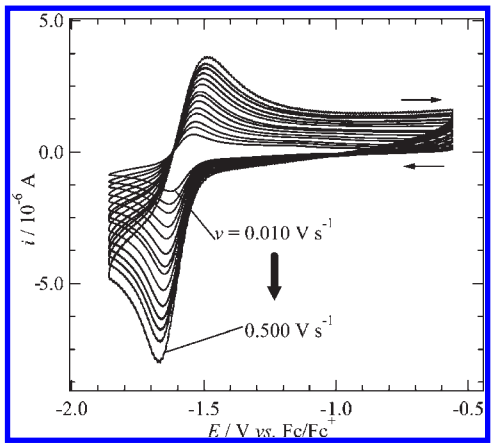

Figure 7. Cyclic voltammograms of $U^{VI}O_2$(saldien) (1.52×10^{-3} M) in DMSO containing 0.106 M TBAP at different potential sweep rates (ν = 0.010−0.500 V·s^{-1}). Initial scan direction: cathodic.

with the coordinating O and N atoms of saldien^{2-}; i.e., there is no space for additional solvent coordination. In addition, no significant enhancement of the peak intensity due to the presence of the S atom of DMSO was detected around 3.6−3.7 Å. These EXAFS results conclude that no solvent coordination occurs even in the strongly Lewis-basic aprotic solvents.

We have not tested the influence of other strong Lewis bases such as the fluoride anion[31] so far. However, any additional unidentate ligands would be very hard to get to interact with $U^{VI}O_2$(saldien) because of its highly crowded equatorial plane. As a matter of fact, the distances between phenolate oxygen atoms of the coordinating saldien^{2-} are 3.11 Å (**1a**), 3.10 Å (**1b**), and 3.14 Å (**1c**), while the sum of van der Waals radii of 2 oxygen atoms is 3.04 Å (2 × 1.52 Å).[25] This implies that there is not enough space as an additional sixth coordination site in $U^{VI}O_2$(saldien).

3.2. Electrochemistry and Spectroelectrochemistry. Cyclic voltammograms of $U^{VI}O_2$(saldien) (1.52×10^{-3} M) in DMSO containing 0.106 M TBAP are shown in Figure 7. The electrochemical data from Figure 7 are listed in Table S4 (Supporting Information). Cathodic and anodic peaks were observed at −1.65 V (E_{pc}) and −1.52 V (E_{pa}) vs Fc/Fc$^+$, respectively. The peak potential separation tends to increase from 0.080 to 0.170 V with increasing potential sweep rate (ν, 0.010−0.500 V·s^{-1}), indicating a quasireversible system. The multiple scanned cyclic voltammogram recorded at each ν showed no differences from Figure 7. Therefore, the reduction product at E_{pc} is reoxidized to $U^{VI}O_2$(saldien) at E_{pa}, and no successive reactions follow both reduction and oxidation. The formal potential [$E^{\circ\prime} = (E_{pc} + E_{pa})/2$] is -1.582 ± 0.005 V vs Fc/Fc$^+$ and constant regardless of ν. Using the current values at E_{pc} (i_{pc}) and the $i_{pc} - \nu^{1/2}$ relationship for the irreversible system,[5a,32] the diffusion coefficient of $U^{VI}O_2$(saldien) in this system was estimated as 2.3×10^{-6} cm^2·s^{-1} at 298 K.

To determine the electron stoichiometry (n) of the redox reaction observed in Figure 7 quantitatively, a UV−vis−NIR spectroelectrochemical experiment was performed for $U^{VI}O_2$(saldien) (4.20×10^{-3} M) in DMSO containing 0.305 M TBAP by using the OTTLE cell. The absorption spectra were recorded at the potentials varied stepwise in the range from −1.392 to −1.792 V vs Fc/Fc$^+$. The resulting spectra are shown in Figure 8 together with that of initial $U^{VI}O_2$(saldien) without the potential application. The spectral changes were observed with a decrease in the potential and converged at −1.792 V vs Fc/Fc$^+$. Isosbestic points were clearly observed at 349, 401, and 544 nm, indicating that only the redox equilibrium of $U^{VI}O_2$(saldien) takes place. Using the absorbance at 373 nm, which is the absorption maximum of the reductant, the concentrations of the oxidant (C_O, here $U^{VI}O_2$(saldien)) and reductant (C_R) at each potential was calculated. The potential value E was plotted as a function of natural logarithm of C_O/C_R in Figure S12 (Supporting Information). From this $E-\ln(C_O/C_R)$ plot, a regression analysis of the following Nernstian equation, eq 1, was performed:

$$E = E^\circ + (RT/nF)\ln(C_O/C_R) \quad (1)$$

where E°, R, T, and F are the standard redox potential, the gas constant (8.314 kJ·mol^{-1}·K^{-1}), the absolute temperature (here 298 K), and the Faraday constant (96485 C·mol^{-1}), respectively. The slope and intercept of the best fit line of eq 1 to the plot in Figure S12 (Supporting Information) were 0.0276 and −1.584, respectively. From the slope, the electron stoichiometry n was calculated as 0.929, which is regarded as unity. Consequently, the product of reduction of $U^{VI}O_2$(saldien) in Figures 7 and 8 is shown to be that of the corresponding U^V complex, [U^VO_2(saldien)]$^-$. From the intercept, E° of [U^VO_2(saldien)]$^-$/$U^{VI}O_2$(saldien) is −1.584 V vs Fc/Fc$^+$, which is in agreement with $E^{\circ\prime}$ from the CV experiment. The most important finding is the fact that [U^VO_2(saldien)]$^-$ is stable in DMSO. This is the third system of the stable U^V complex in a nonaqueous system we have found. The electronic spectrum recorded at −1.792 V vs Fc/Fc$^+$ is assigned to pure [U^VO_2(saldien)]$^-$ in DMSO.

The electronic spectrum of [U^VO_2(saldien)]$^-$ in DMSO is shown in Figure 9. The transverse axis was converted from wavelength (nm) to wavenumber (cm^{-1}). The peak maxima of the characteristic absorption bands of [U^VO_2-(saldien)]$^-$ were observed at 5260, 7250, 12 000, 14 300, 15 900, and 26 800 cm^{-1}, which correspond to 1890, 1390, 830, 700, 630, and 373 nm, respectively. Because of the strong intensity at 26 800 cm^{-1} with a molar absorptivity (ε) = ca. 13 000 M^{-1}·cm^{-1}, this absorption band can be assigned to an electric-dipole allowed transition arising from the coordinating saldien^{2-} and/or from charge-transfer between U and saldien^{2-}. In contrast, the ε values of the absorption bands at $<$20 000 cm^{-1} are relatively small, 100−400 M^{-1}·cm^{-1}, suggesting that these electronic transitions are essentially forbidden. Furthermore, the absorption spectrum of [U^VO_2(saldien)]$^-$ in the vis−NIR regions is similar to those of the other U^V complexes in the pentagonal bipyramidal ligand field ([U^VO_2(salophen)-DMSO]$^-$ and [U^VO_2(dbm)$_2$DMSO]$^-$),[5a,d] indicating that these absorption bands arise from the electronic transitions

(31) (a) Cametti, M.; Nissinen, M.; Dalla Cort, A.; Mandolini, L.; Rissanen, K. *Chem. Commun.* **2003**, 2420–2421. (b) Cametti, M.; Nissinen, M.; Dalla Cort, A.; Mandolini, L.; Rissanen, K. *J. Am. Chem. Soc.* **2005**, *127*, 3831–3837. (c) Cametti, M.; Nissinen, M.; Dalla Cort, A.; Rissanen, K.; Mandolini, L. *Inorg. Chem.* **2006**, *45*, 6099–6101. (d) Cametti, M.; Nissinen, M.; Dalla Cort, A.; Mandolini, L.; Rissanen, K. *J. Am. Chem. Soc.* **2007**, *129*, 3641–3648. (e) Cametti, M.; Dalla Cort, A.; Mandolini, L.; Nissinen, M.; Rissanen, K. *New J. Chem.* **2008**, *32*, 1113–1116.

(32) (a) Heinze, J. *Angew. Chem., Int. Ed.* **1984**, *23*, 831–847. (b) Nicholson, R. S.; Shain, I. *Anal. Chem.* **1964**, *36*, 706–723.

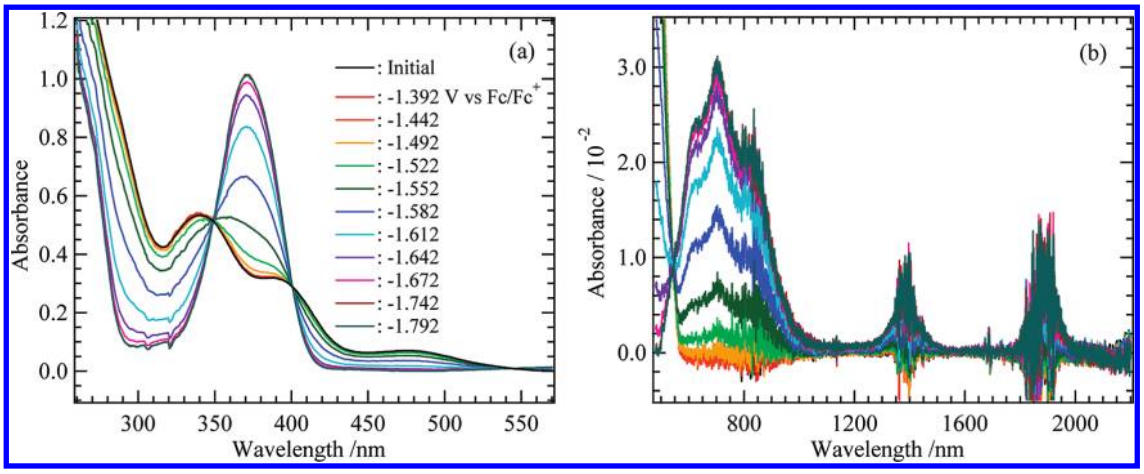

Figure 8. Electronic spectra recorded at the applied potentials in the range from −1.392 to −1.792 V vs Fc/Fc^+ for $U^{VI}O_2$(saldien) (4.20×10^{-3} M) in DMSO containing 0.305 M TBAP. Wavelength regions: (a) 260−570 nm, (b) 480−2200 nm. Noises are due to detectors (photomultiplier and PbS detector) in the spectrophotometer and/or absorption of DMSO in the OTTLE cell. Optical path length: 1.89×10^{-2} cm.

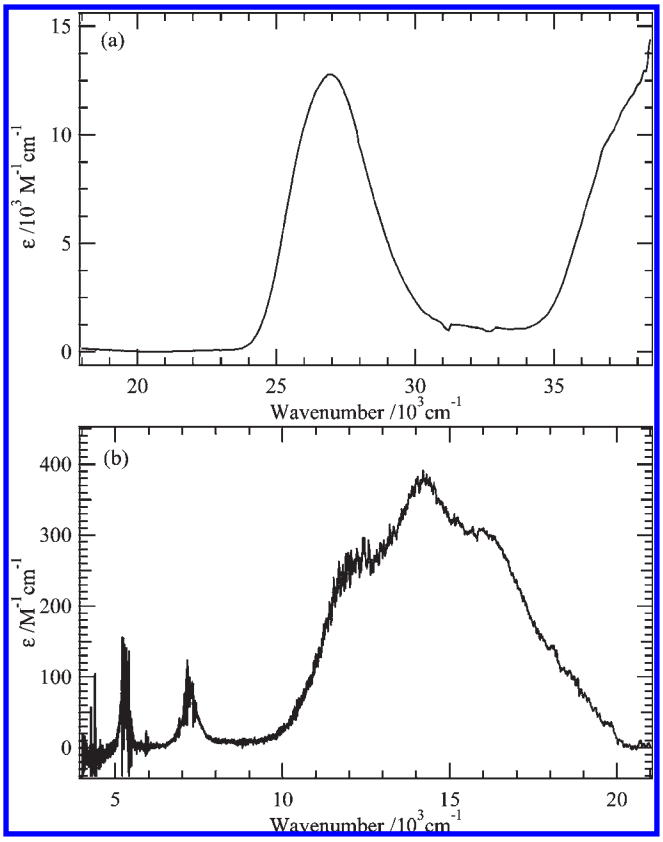

Figure 9. Electronic spectrum of $[U^VO_2(saldien)]^-$ in DMSO. Energy ranges: (a) 18000−38000 cm^{-1} (555−263 nm), (b) 4000−21000 cm^{-1} (2500−476 nm).

in a $U^VO_2^+$ core. In accordance with our previous discussion[5d] and the later theoretical calculation by Ruipérez et al.,[33] the absorption band at 15 900 cm^{-1} is attributable to charge transfer from O_{ax} to U^{5+}, and the others at 5260, 7250, 12 000, and 14 300 cm^{-1} are assigned to f−f transitions in the $5f^1$ configuration of U^{5+}. It should be noted that both transitions occur between the energy states with the same parity (here, ungerade) and are therefore electric-dipole forbidden essentially.

In a bare $U^VO_2^+$, U $5f\delta_u$ and $5f\phi_u$ orbitals do not participate in any bond formation but stay as degenerate nonbonding orbitals.[34] When an equatorial coordination is formed, $5f\phi_u$ with six lobes localized on the *xy* plane participate in the interaction with the coordinating atoms of the ligand, having an antibonding character. In contrast, $5f\delta_u$ is still nonbonding because its lobes are neither lying on the *xy* plane nor present directly along any bonds. Thus, the unpaired electron in U^{5+} will occupy the nonbonding $5f\delta_u$ in the actual U^V complexes, although the spin−orbit coupling in the $5f^1$ configuration actually has to be taken into account for the detailed discussion. In summary, the energy order of the 5f orbitals in a U^V complex is predicted to be $5f\sigma_u$ ($^2\Sigma_u$)≫$5f\pi_u$ ($^2\Pi_u$) > $5f\phi_u$ ($^2\Phi_u$) > $5f\delta_u$ ($^2\Delta_u$).[35] Among them, it is generally accepted that the $^2\Sigma_u$ state is located at much higher energy than others.[36] Therefore, the electronic transition to $^2\Sigma_u$ may be ruled out from the present discussion. Further splitting of $^2\Pi_u$, $^2\Phi_u$, and $^2\Delta_u$ into $^2\Pi_{1/2u}$, $^2\Pi_{3/2u}$, $^2\Phi_{5/2u}$, $^2\Phi_{7/2u}$, $^2\Delta_{3/2u}$, and $^2\Delta_{5/2u}$ arises from the spin−orbit coupling; i.e., five electronic transitions are observable in total. Since participation of $5f\pi_u$ in the $U-O_{ax}$ bond is much stronger than that of $5f\phi_u$ in the equatorial coordination, the absorption bands due to the electronic transitions to the $^2\Pi_u$ states would be broader than those to $^2\Phi_u$. The transition to $^2\Delta_u$ would also show the narrow absorption bands because of the lesser participation of $5f\delta_u$ in the chemical bonding. Although the precise energy order of $^2\Phi_{5/2u}$, $^2\Phi_{7/2u}$, and $^2\Delta_{5/2u}$ cannot be concluded from the obtained experimental data, the narrower absorption bands at 5260 and 7250 cm^{-1} are assigned to two of the transitions from the $^2\Delta_{3/2u}$ ground state to $^2\Delta_{5/2u}$ and/or $^2\Phi_u$ excited states. The first excited state of the f−f transition in U^V and isoelectronic Np^{VI} species is lying at 100−1000 cm^{-1},[33,36,37] which is outside of the detection range in usual absorption

(33) Ruipérez, F.; Danilo, C.; Réal, F.; Flament, J.-P.; Vallet, V.; Wahlgren, U. *J. Phys. Chem. A* **2009**, *113*, 1420–1428.

(34) Matsika, S.; Zhang, Z.; Brozell, S. R.; Blaudeau, J.-P.; Wang, Q.; Pitzer, R. M. *J. Phys. Chem. A* **2001**, *105*, 3825–3828.

(35) Term symbols of the energy states in an actual U^V complex should be expressed by using Mulliken symbols for an appropriate point group. However, it is not easy to suppose which 5f orbital participates in an energy state discussed. In this article, we did use the symbols in $D_{\infty h}$ for simplicity of discussion.

(36) Denning, R. G.; Norris, J. O. W.; Brown, D. *Mol. Phys.* **1982**, *46*, 287–323.

(37) Matsika, S.; Pitzer, R. M. *J. Phys. Chem. A* **2000**, *104*, 4064–4068.

spectroscopic experiments. The broader absorption bands at 12 000 and 14 300 cm^{-1} are attributed to the transitions to the $^2\Pi_u$ excited states. Furthermore, it is obvious that the pentagonal equatorial coordination cannot be constructed only from any combinations of the 5f orbitals. Additional participation of 6d orbitals which have even parity (gerade) can be expected, i.e., 6d−5f hybridization.[38] This may explain from where the intensity of the f−f transitions in U^V complexes with the pentagonal bipyramidal ligand field arises. Thus, such a transition in the U^V complexes has no longer a pure f−f nature, but the characters of the electric-dipole allowed d−f and f−d transitions are incorporated to a certain extent.

According to Bart et al.,[39] a monooxo U^V complex, $(('BuArO)_3tacn)U^VO$, shows four sharp absorption bands [5650, 6769, 8300, and 11 765 cm^{-1} (1770, 1480, 1205, and 850 nm, respectively)] and one shoulder [17 100 cm^{-1} (585 nm)] at a similar position to our dioxo U^V complexes reported here and previously.[5d] The similarity is also found in the relatively high molar absorptivities of the essentially electric-dipole forbidden transitions (20−90 $M^{-1}\cdot cm^{-1}$) under a lack of a center of inversion, which destroys the Laporte selection rule. The most significant difference between their monooxo U^V and our dioxo one is the width of the absorption bands in the range from 8000 to 20 000 cm^{-1} (1250−500 nm). As described above, two of the broad absorption bands of the dioxo U^V complexes in the lower energy are attributable to the transitions to the $^2\Pi_u$ excited states. The $5f\pi_u$ orbitals participate in the π-type bond formation between U and O_{ax}, and the degree of this participation in the dioxo species is predicted to be stronger than that in the monooxo one. This may explain the difference in the absorption band widths and support our assignment for these bands. Regarding the transition energies to the $^2\Pi_u$ excited states, the absorption bands of the dioxo U^V complexes with the pentagonal equatorial plane are actually blue-shifting from those of the monooxo species by 2000−4000 cm^{-1}. On the other hand, the corresponding transition energies of $U^VO_2(CO_3)_3^{5-}$ with a hexagonal equatorial plane are 8770 and 10 100 cm^{-1}, which are close to those of the monooxo U^V in spite of its dioxo form. Any explanation for this concern is not given so far.

4. Conclusion

In the present study, we investigated the molecular structure of $U^{VI}O_2$(saldien) in the solid and solution states. Our strategy to prevent the cation−cation interaction (CCI) and to preserve a stable U^V species is the full chelation of the equatorial coordination sites of the $U^VO_2^+$ ion using a chelating pentadentate ligand, $saldien^{2-}$. As expected, this ligand does not allow the solvent molecule L to participate in the U^{VI} coordination sphere even in strongly Lewis-basic solvents, DMSO and DMF. The electrochemical behavior of $U^{VI}O_2$(saldien) in DMSO was also studied by the cyclic voltammetry and UV−vis−NIR spectroelectrochemical technique. Consequently, we found the new stable U^V complex $[U^VO_2(saldien)]^-$ in DMSO. This U^V complex shows the characteristic absorption bands due to f−f transition in the $5f^1$ configuration and charge-transfer from O_{ax} to U^{5+} in the vis−NIR regions, which can be regarded as a common character of U^V complexes. In summary, the CCI formation was successfully prevented by the saturation of the equatorial coordination sites using $saldien^{2-}$, as we expected, and the U^V species is stabilized by a fully chelating equatorial coordination sphere. The use of other ligand sets, e.g., pentadentate superphthalocyanine[14] as described in the Introduction, a combination of tridentate and bidentate ligands ("3 + 2" type complex), and hexadentate macrocycles,[40] may also have the potential to hamper the CCI formation and hence to stabilize a U^V complex.

Acknowledgment. S.T. was supported by a stipend from the Alexander von Humboldt foundation. This work was partly supported by the Deutsche Forschungsgemeinschaft under contract HE 2297/2-2.

Supporting Information Available: CIF of **1a**−**c**. *J*-coupling scheme in the $N-CH_2CH_2-NH-CH_2CH_2-N$ moiety in $U^{VI}O_2$(saldien), packing diagrams of **1a**−**c**, specific intermolecular interactions in crystal lattices of **1a**−**c**, ^1H NMR spectra of DMSO-d_6 solution dissolving **1a** and **1c**, $^1H-^1H$ COSY diagram of DMSO-d_6 solution of **1a**, *J*-coupling simulation for ^1H NMR spectrum of **1a** in DMSO-d_6, Nernstian plot for Figure 8, table of coupling constants in *J*-coupling, table of structural parameters from EXAFS curve fit for $U^{VI}O_2$(saldien) in DMSO, and table of electrochemical data of $U^{VI}O_2$(saldien) in DMSO. This material is available free of charge via the Internet at http://pubs.acs.org.

(38) Mizuoka (Takao), K. Ph.D. thesis, Tokyo Institute of Technology, **2006**. Available as a PDF file on request. Contact: k.takao@fzd.de (K.T.) or yikeda@nr.titech.ac.jp (Y.I.)

(39) Bart, S. C.; Anthon, C.; Heinemann, F. W.; Bill, E.; Edelstein, N. M.; Meyer, K. *J. Am. Chem. Soc.* **2008**, *130*, 12536–12546.

(40) For example: (a) Bauer, V. J.; Clive, D. L. J.; Dolphin, D.; Paine, J. B., III; Harris, F. L.; King, M. M.; Loder, J.; Wang, S.-Y. C.; Woodward, R. B. *J. Am. Chem. Soc.* **1983**, *105*, 6429–6436. (b) De Cola, L.; Smailes, D. L.; Vallarino, L. M. *Inorg. Chim. Acta* **1985**, *110*, L1–L2. (c) Van Staveren, C. J.; Van Eerden, J.; Van Veggel, F. C. J. M.; Harkema, S.; Reinhoudt, D. N. *J. Am. Chem. Soc.* **1988**, *110*, 4994–5008. (d) Benetollo, F.; Bombieri, G.; De Cola, L.; Polo, A.; Smailes, D. L.; Vallarino, L. M. *Inorg. Chem.* **1989**, *28*, 3447–3452. (e) Sessler, J. L.; Mody, T. D.; Lynch, V. *Inorg. Chem.* **1992**, *31*, 529–531. (f) Sessler, J. L.; Mody, T. D.; Dulay, M. T.; Espinoza, R.; Lynch, V. *Inorg. Chim. Acta* **1996**, *246*, 23–30. (g) Casellato, U.; Tamurini, S.; Tomasin, P.; Vigato, P. A. *Inorg. Chim. Acta* **2002**, *341*, 118–126. (h) Sessler, J. L.; Callaway, W. B.; Dudek, S. P.; Date, R. W.; Bruce, D. W. *Inorg. Chem.* **2004**, *43*, 6650–6653.